Gu et al. Nanoscale Research Letters (2019) 14:40
https://doi.org/10.1186/s11671-019-2872-7

Nanoscale Research Letters

NANO EXPRESS Open Access

Recovery Performance of Ge-Doped Vertical GaN Schottky Barrier Diodes

Hong Gu[1,2], Feifei Tian[3], Chunyu Zhang[3], Ke Xu[3], Jiale Wang[1], Yong Chen[1], Xuanhua Deng[1] and Xinke Liu[1*]

Abstract

Vertical GaN Schottky barrier diodes (SBDs) were fabricated on Ge-doped free-standing GaN substrates. The crystal quality of the SBDs was characterized by cathode luminescence measurement, and the dislocation density was determined to be ~ 1.3×10^6 cm^{-2}. With the electrical performance measurements conducted, the SBDs show a low turn-on voltage V_{on} (0.70~0.78 V) and high current I_{on}/I_{off} ratio (9.9×10^7~1.3×10^{10}). The reverse recovery characteristics were investigated. The reverse recovery time was obtained to be 15.8, 16.2, 18.1, 21.22, and 24.5 ns for the 100-, 200-, 300-, 400-, and 500-μm-diameter SBDs, respectively. Meanwhile, the reverse recovery time and reverse recovery charge both show a significant positive correlation with the electrode area.

Keywords: Vertical SBDs, Ge-doped GaN substrates, Reverse recovery time, HVPE

Introduction

Recently, a wide band gap semiconductor—such as GaN—with the inherent advantages, has attracted tremendous research attention for the next-generation electronics devices, particularly in the field of high frequency, high power, and high performance [1–6]. Meanwhile, thanks to the developments of hydride vapor phase epitaxy (HVPE), low dislocation density (≤ 10^6 cm^{-2}) GaN substrates are now commercially available [7–10]. Compared with lateral devices, vertical-type devices fabricated with these substrates are considered to be a more advanced structure which is conducive to achieving a larger current, less leakage path, and better reliability for the system [11, 12]. Among them, GaN-based Schottky barrier diode (SBD) is a vital component in the switching devices. Differed from a bipolar diode, the SBD with its unipolar nature greatly reduces the minority carrier storage effect and correspondingly offers a high switching speed with low reverse recovery loss. However, few groups have conducted a systematic study of the reverse recovery characteristics for vertical GaN SBDs [13–17], of which studies focused more on the comparison of the switching time in different structures devices. Thus, there is still an urgent need of a deep investigation into the mechanism of recovery performance for GaN SBDs, especially for the vertical ones.

Meanwhile, since the ohmic contact technique has been continuously explored to improve device performance in many published papers [18], heavily doped n-type GaN is a key link for fabricating nitride devices. Lately, Ge is proposed as an alternative to Si dopant in GaN, because both of them share a similar characteristic of shallow level impurity (the activation energy is reported to be 20 and 17 meV for Ge and Si, respectively) and the lattice distortion caused by Ge atoms substituting into Ga sites would be smaller owing to their closer ionic radii [19, 20]. The Ge doping is believed to form a smoother surface with fewer defects [21, 22]. Moreover, with the lower lattice distortion and film stress, this doping also shows a promise in high-temperature electronic devices that put more emphasis on the thermal stability. Although the Ge-doped GaN has been studied theoretically, it is essential to investigate the real impact on the relevant device. In this paper, the novel vertical GaN SBDs fabricated on Ge-doped free-standing (FS) GaN substrate are proposed. The vertical GaN SBDs exhibit a superior crystal quality and electronic property. Meanwhile, the recovery performance of vertical SBDs is systematically investigated. The reverse recovery time and reverse recovery charge finally show a significant positive correlation with the electrode area.

* Correspondence: xkliu@szu.edu.cn
[1]College of Materials Science and Engineering, Guangdong Research Center for Interfacial Engineering of Functional Materials, Shenzhen Key Laboratory of Special Functional Materials, Chinese Engineering and Research Institute of Microelectronics, Shenzhen University, Shenzhen 518060, People's Republic of China
Full list of author information is available at the end of the article

Springer Open

© The Author(s). 2019 **Open Access** This article is distributed under the terms of the Creative Commons Attribution 4.0 International License (http://creativecommons.org/licenses/by/4.0/), which permits unrestricted use, distribution, and reproduction in any medium, provided you give appropriate credit to the original author(s) and the source, provide a link to the Creative Commons license, and indicate if changes were made.

Methods and Experiments

The schematic of device structures for the fabricated SBDs is displayed in Fig. 1a, which mainly consists of a 390-μm FS n^+-GaN substrate and a 9-μm n^--GaN drift layer. In this work, the (0001)-oriented GaN substrate layer with a Ge concentration of 1×10^{18} cm^{-3} and a dislocation density of 1×10^{6} cm^{-2} was grown by HVPE. And the undoped epitaxial layer on this substrate was grown by metalorganic chemical vapor deposition, with a growth rate of ~ 2 μm/h. For SBD fabrication, Ti/Al/Ni/Au ohmic contacts were formed on the back surface of the GaN substrate. Ni/Au Schottky electrodes were formed on the front surface of the epitaxial layer with five different diameters (100, 200, 300, 400, and 500 μm), as shown in Fig. 1b. More information about the fabrication process can be found in our previous report [23, 24].

The cathodoluminescence (CL) images were obtained using a Quanta 400 FEG scanning electron microscope (SEM) with a 10-kV accelerating voltage to study the spatial distribution of dislocation density for the epitaxial layer. Capacitance-voltage (*C-V*) and current-voltage (*I-V*) measurements were performed using a Keithley 4200 semiconductor parameter analyzer to evaluate electronic properties of the SBDs. And temperature-dependent measurements were conducted in the range of 300 to 500 K with a customized experimental setup.

Results and Discussion

The CL result of the epitaxial layer is presented in Fig. 1c. As the dislocation is believed to be a nonradiative recombination center, it appears on the CL image in the form of a dark spot. Since no noticeable spatial distribution difference is observed, the average value of dislocation density was calculated to be ~ 1.3×10^{6} cm^{-2}, with the CL measurements performed at several different regions. This result indicates a high-quality epitaxial layer was obtained for vertical SBDs.

As the vertical SBDs were characterized in a parallel mode, the *C-V* and *G-V* curves were obtained with 1 MHz frequency. The results of the SBDs are shown in Fig. 2a and b, respectively, where ($1/C^2$) versus applied voltage V is plotted in the inset. Here, carrier concentration N_d could be evaluated with the expression: $N_d = \frac{-2}{A^2 q\varepsilon[d(1/C^2)/dV]}$, where A is the area of Schottky electrodes, q is the electron charge (1.602×10^{-19} C), and ε is the dielectric constant of GaN (8.854×10^{-11} F/m). Hence, the N_d of the epitaxial layer was determined to be ~ 6.2×10^{15} cm^{-3}. And the phase angle θ also could be calculated by the following equation: $\theta = \tan^{-1}\left(\frac{2\pi fC}{G}\right)$, where f is the applied frequency, C is the capacitance, and G is the measured conductance (gate leakage). Since the results for different diameters are similar, the calculated angle θ versus applied voltage V of the 300-μm-diameter SBDs is shown in the inset of Fig. 2b as an example. Note that the θ is very close to 90°, it confirms that an excellent Schottky gate with a low leakage path is achieved in this study. The *J-V* characteristics are also presented in Fig. 2c. It is clearly seen that the I_{on}/I_{off} ratios are 3.8×10^9, 5.9×10^8, 1.3×10^{10}, 6.5×10^8, and 9.9×10^7 for the 100-, 200-, 300-, 400-, and 500-μm-diameter SBDs, respectively, of which the I_{on} and I_{off} are defined as the current at the gate voltage of 1.6 and − 2 V, respectively. After linear fitting, the turn-on voltage V_{on} of vertical SBDs is determined to be 0.70, 0.76, 0.72, 0.70, and 0.78 V, respectively, with the electrode diameters increasing from 100 to 500 μm. These results indicate a good electronic property was obtained for the vertical SBDs.

A typical test circuit was used to measure the reverse recovery characteristics of the vertical SBDs, as shown in Fig. 3a. The periodic square wave voltage signals (from

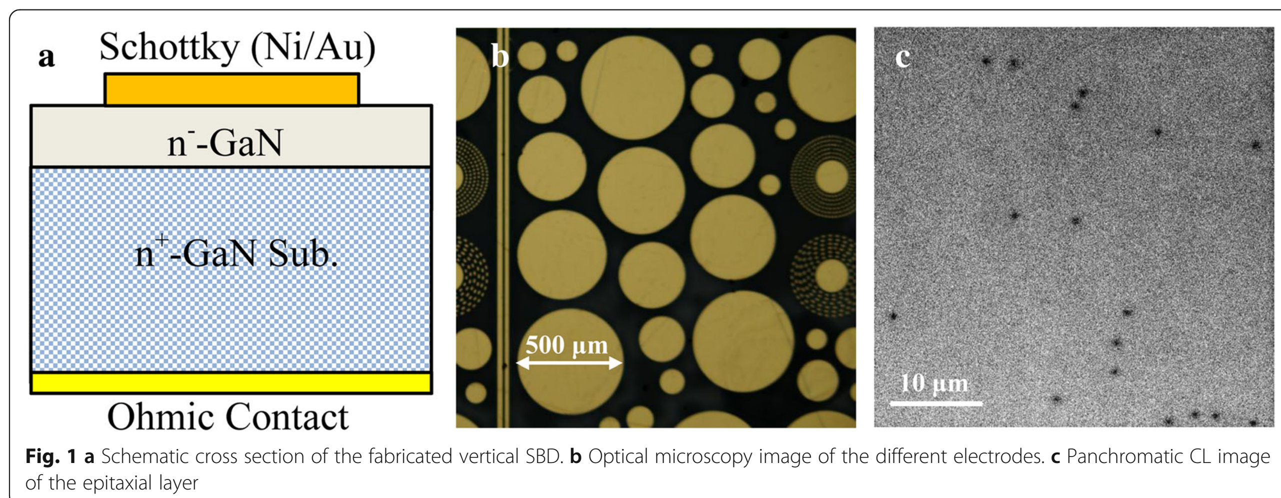

Fig. 1 **a** Schematic cross section of the fabricated vertical SBD. **b** Optical microscopy image of the different electrodes. **c** Panchromatic CL image of the epitaxial layer

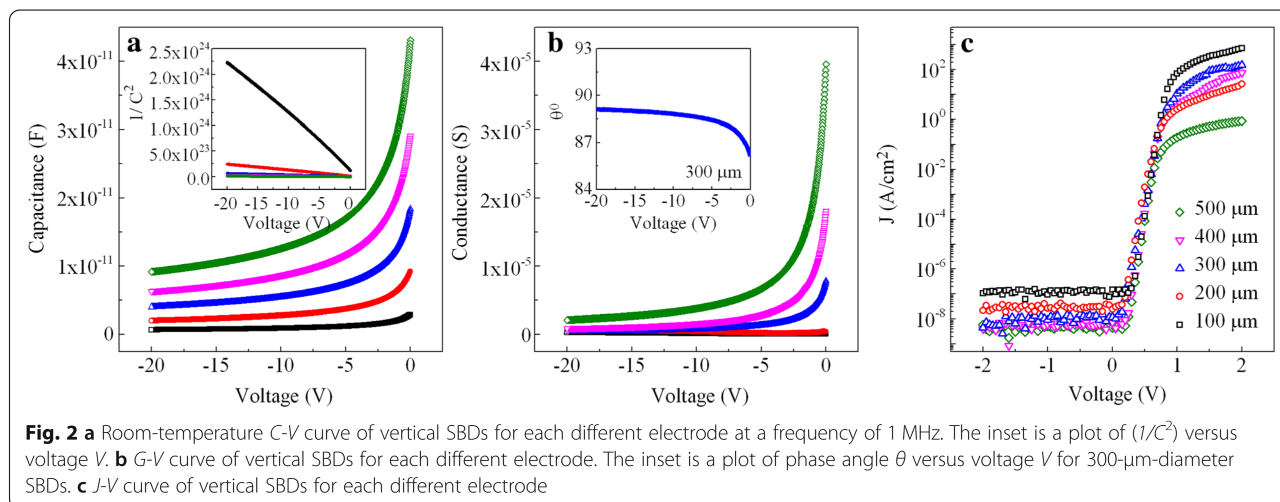

Fig. 2 **a** Room-temperature *C-V* curve of vertical SBDs for each different electrode at a frequency of 1 MHz. The inset is a plot of ($1/C^2$) versus voltage *V*. **b** *G-V* curve of vertical SBDs for each different electrode. The inset is a plot of phase angle θ versus voltage *V* for 300-μm-diameter SBDs. **c** *J-V* curve of vertical SBDs for each different electrode

+ 20 to − 20 V) were applied sequentially to a device under test (DUT), where a parasitically inductor would store the magnetic energy and affect the current. When the voltage signal changed, an oscillation current may take place during the period. A high-speed current probe with a Tektronix MDO 4104-3 oscilloscope was disposed for detecting the transient current variation in the vertical SBDs. As the schematic waveform of reverse recovery current is shown in Fig. 3b, in this study, t_a is defined as the storage time while t_b is defined as the reverse current delay time. And the reverse recovery time T_{rr} is defined as the time when the reverse current recovers to 10% of the maximum reverse recovery current I_{RM}, which is the sum of t_a and t_b. And the reverse recovery charge Q_{rr} is obtained by integrating the reverse current until T_{rr} which corresponds to the accumulated charge in a diode.

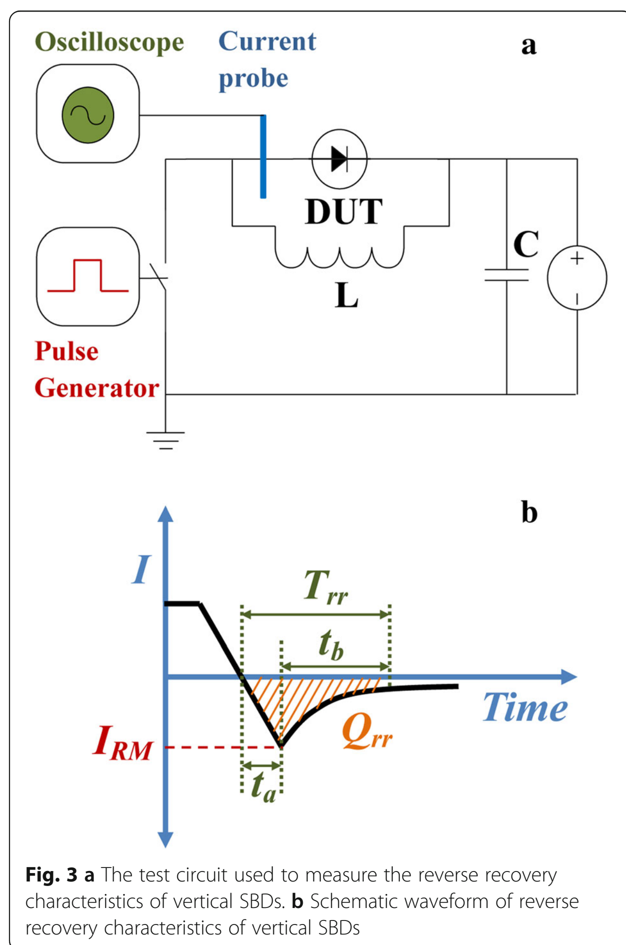

Fig. 3 **a** The test circuit used to measure the reverse recovery characteristics of vertical SBDs. **b** Schematic waveform of reverse recovery characteristics of vertical SBDs

Figure 4 shows the reverse recovery curve of vertical SBDs for each electrode diameter when the applied voltage switched from + 20 to − 20 V. Here, for the 100-, 200-, 300-, 400-, and 500-μm-diameter SBDs, the T_{rr} values were obtained to be 15.8, 16.2, 18.1, 21.22, and 24.5 ns, while the Q_{rr} values were integrated to be 0.0127, 0.0536, 0.150, 0.280, and 0.405 nC, respectively. These vertical devices all exhibited a fast switching time (less than 25 ns). A considerable low reverse current is also observed in the results, which could be due to the smaller amount of stored charge in the SBDs [13]. Meanwhile, it is also clearly seen that the value of T_{rr} and Q_{rr} both increase together with the enlarging of electrode diameters, and the smallest one shows the fastest T_{rr} of 15.8 ns.

To further investigate the mechanism underlying those changes, the vertical SBDs were also measured when the voltage switched from + 10 to − 10 V. As the reverse recovery time T_{rr} versus the diode diameter d is plotted in Fig. 5, the value of T_{rr} for each diode was not noticeably altered. The reverse recovery charge Q_{rr} versus the d is displayed in Fig. 6 simultaneously, where the data of two curves point toward the same trend. Meanwhile, it is notable that the Q_{rr} of both tests show a significant positive correlation with the d^2, that is, the electrode area.

In fact, it is reported that the reverse recovery effect should be mainly from the parasitic inductance and interface trapping of SBDs [25, 26]. Considering that the

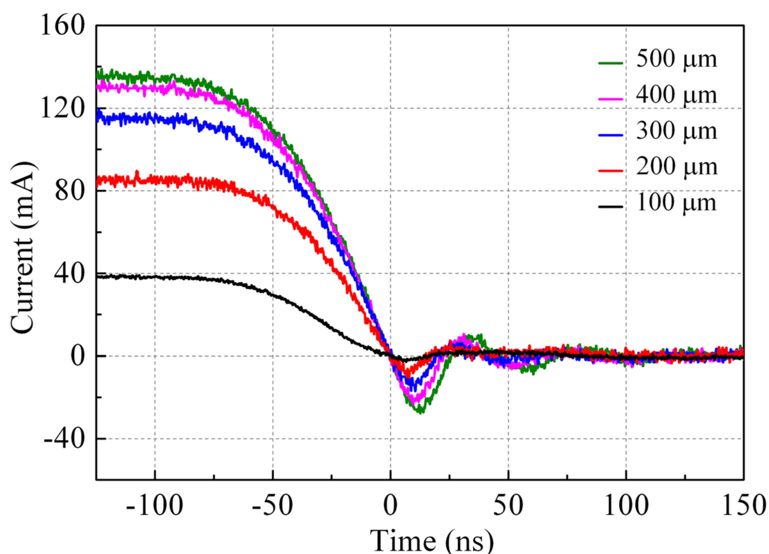

Fig. 4 Reverse recovery current of vertical SBDs for each different electrode

contribution of parasitic inductance is characterized in the form of oscillation current which is not obviously observed in these reverse recovery curves, thus, the changing of reverse recovery time and reverse recovery charge should have resulted from the traps [27, 28]. Since the concentration of traps is uniform in vertical SBDs, the Q_{rr} would depend on the contact area of the device and finally increase with the electrode area as shown in Fig. 6. Thus, the traps act as an electric field stopper in the interface. During the t_a period, the delay was strongly influenced by carrier trapping in the Schottky junction, while in the t_b period, reverse recovery speed is also slowed by the time for sweeping the stored charge out of the junction. These results are consistent with our previous report [29], which suggested the *RC* time constant increases with the increase of device diameter and shows a good dependency with the reverse recovery time. And a further improvement of reverse recovery characteristics could be expected from a smaller electrode or thinner drift layer in these devices.

Moreover, the recovery performance of vertical SBDs is further investigated in a higher temperature. Figure 7 shows reverse recovery current for 500-μm-diameter GaN SBDs which were measured at 300, 400, and 500 K, respectively. Neither the reverse recovery time nor reverse

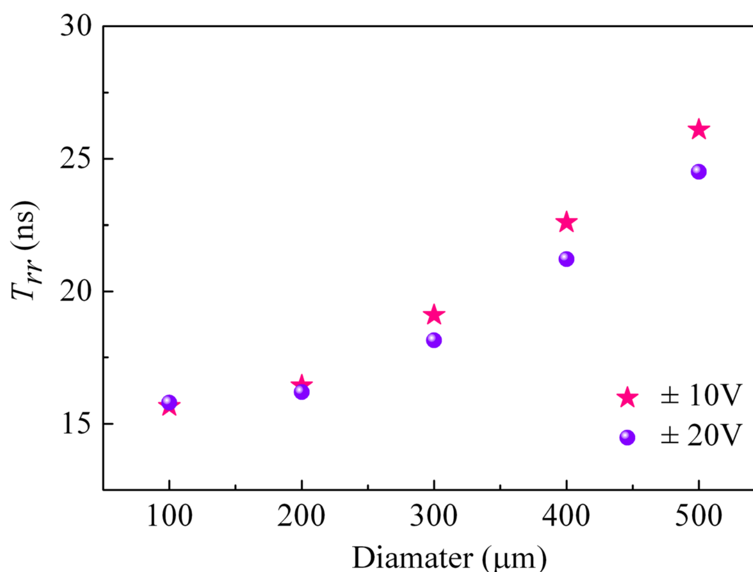

Fig. 5 Reverse recovery time T_{rr} versus electrode diameter *d*

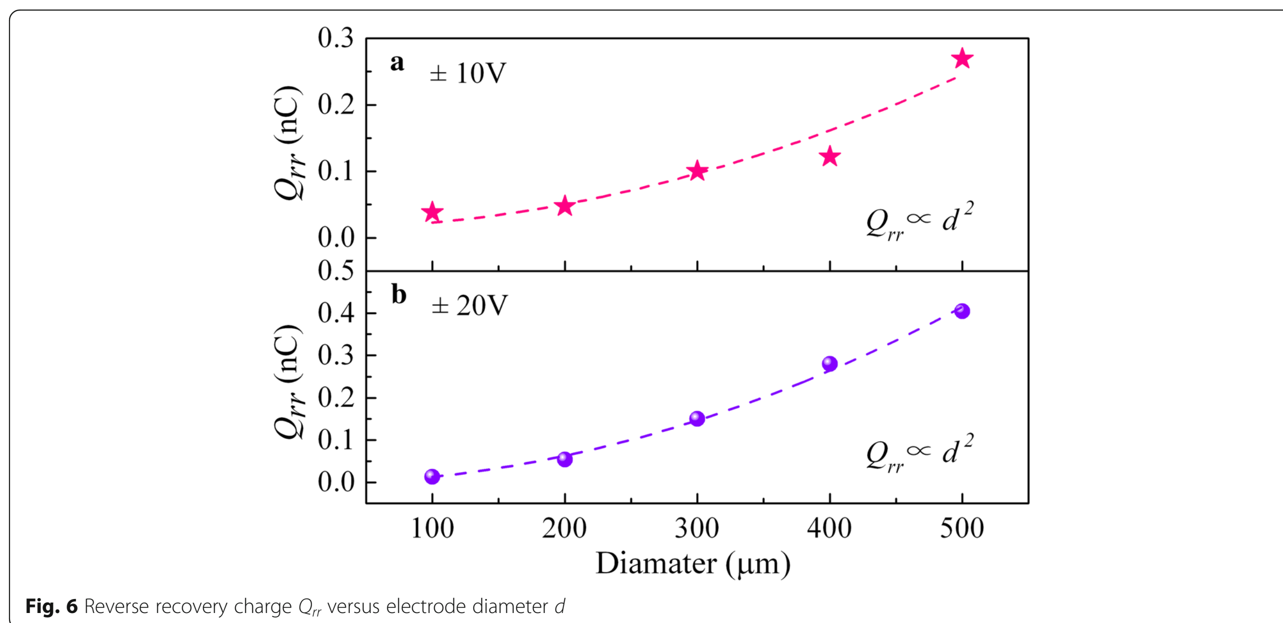

Fig. 6 Reverse recovery charge Q_{rr} versus electrode diameter d

recovery charge is observed changed with the temperature rising. These results are consistent with the above analysis, as the concentration of trap is not very sensitive to the temperature. Conversely, it is reported that the reverse recovery time of Si-based SBDs would increase by 191% as the temperature rises from 300 to 425 K [17]. Here, with a short carrier lifetime and wider bandgap, GaN SBDs are shown to provide substantial improvements in current-handling capability, reverse recovery, and energy loss. As the thermal stability of GaN-based SBDs is superior than that of traditional narrow bandgap semiconductors [30], it can be concluded that GaN is also a suitable material for switching devices applied to a high-temperature environment.

Conclusions

In summary, we fabricated vertical GaN SBDs on Ge-doped FS GaN substrates grown by HVPE. With the material characterization and current-voltage measurements performed, it indicates that an excellent crystal quality and electronic property was obtained for the vertical SBDs. The reverse recovery characteristics were systematically investigated. The reverse recovery time was obtained to be 15.8, 16.2, 18.1, 21.22, and 24.5 ns for the 100-, 200-,

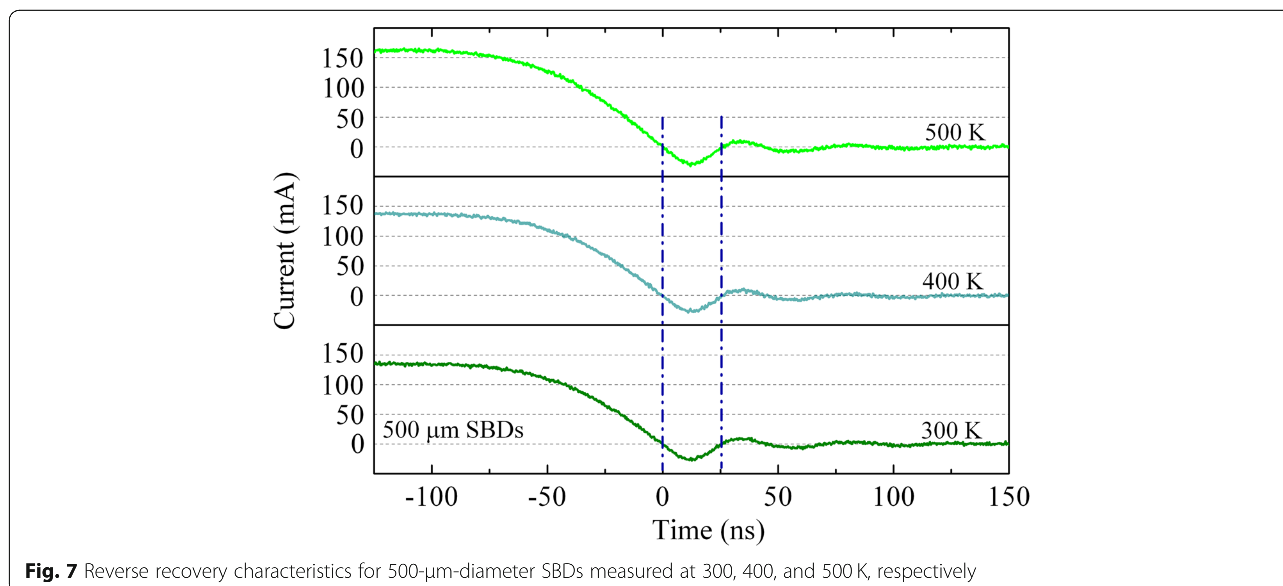

Fig. 7 Reverse recovery characteristics for 500-μm-diameter SBDs measured at 300, 400, and 500 K, respectively

300-, 400-, and 500-μm-diameter diodes, respectively. Meanwhile, the reverse recovery time and reverse recovery charge both show a significant positive correlation with the electrode area. Our results may serve as a reference for further improving the recovery performance of GaN-based SBDs.

Abbreviations
CL: Cathodoluminescence; *C-V*: Capacitance-voltage; DUT: Device under test; FS: Free-standing; GaN: Gallium nitride; HVPE: Hydride vapor phase epitaxy; *I-V*: Current-voltage; SBDs: Schottky barrier diodes; SEM: Scanning electron microscope

Acknowledgements
We acknowledge Photonics Center of Shenzhen University for technical support.

Funding
National Key Research and Development Plan (2017YFB0404100).

Availability of Data and Materials
All data generated or analyzed during this study are included in this published article.

Authors' Contributions
HG, FFT, CYZ, JLW, YC, and XHD carried out the related experiments and data analysis. HG drafted the manuscript. XKL supervised the experiments and the writing of the manuscript. KX provided suggestions and guidance for the experiments and data analysis. All authors read and approved the final manuscript.

Authors' Information
KX is a professor in materials science. XKL is an associate professor in materials physics. HG, FFT and CYZ are associate professors in material characterization. JLW, YC, and XHD are students in fabrication nano-device.

Competing Interests
The authors declare that they have no competing interests.

Publisher's Note
Springer Nature remains neutral with regard to jurisdictional claims in published maps and institutional affiliations.

Author details
[1]College of Materials Science and Engineering, Guangdong Research Center for Interfacial Engineering of Functional Materials, Shenzhen Key Laboratory of Special Functional Materials, Chinese Engineering and Research Institute of Microelectronics, Shenzhen University, Shenzhen 518060, People's Republic of China. [2]Key Laboratory of Optoelectronic Devices and Systems of Ministry of Education and Guangdong Province, College of Optoelectronic Engineering, Shenzhen University, Shenzhen 518060, People's Republic of China. [3]Suzhou Institute of Nano-Tech and Nano-Bionics, CAS, Suzhou 215123, People's Republic of China.

Received: 25 December 2018 Accepted: 20 January 2019
Published online: 31 January 2019

References
1. Del Alamo J, Joh J (2009) GaN HEMT reliability. Microelectron Reliab 49(9–11):1200–1206
2. Chowdhury S, Swenson BL, Wong MH et al (2013) Current status and scope of gallium nitride-based vertical transistors for high-power electronics application. Semicond Sci Technol 28(7):074014
3. Jones A, Wang F, Costinett D (2016) Review of commercial GaN power devices and GaN-based converter design challenges. IEEE Journal of Emerging and Selected topic in power electronics. 4:709-719
4. Liu X, Gu H, Li K et al (2017) AlGaN/GaN high electron mobility transistors with a low sub-threshold swing on free-standing GaN wafer. AIP Adv 7:095305
5. Che J, Chu C, Tian K et al (2018) On the current spreading layer for AlGaN-based deep ultraviolet light-emitting diodes. Nanoscale Res Lett 13:355
6. Kim H, Yoon H, Choi B (2018) Thickness dependence on interfacial and electrical properties in atomic layer deposited AlN on c-plane GaN. Nanoscale Res Lett 13:232
7. Gu H, Ren G, Zhou T et al (2016) The electrical properties of bulk GaN crystals grown by HVPE. J Cryst Growth 436:76–81
8. Gu H, Wu K, Zheng S et al (2018) Redshift of A1(longitudinal optical) mode for GaN crystals under strong electric field. Appl Phys Express 11:011002
9. Gallaghera J, Anderson T, Luna L et al (2019) Long range, non-destructive characterization of GaN substrates for power devices. J Cryst Growth 506:178–184
10. Fu H, Zhang X, Fu K et al (2018) Nonpolar vertical GaN-on-GaN p–n diodes grown on free-standing m-plane GaN substrates. Appl Phys Express 11: 111003
11. Sang L, Ren B, Sumiya M et al (2017) Initial leakage current paths in the vertical-type GaN-on-GaN Schottky barrier diodes. Appl Phys Lett 111: 122102
12. Ren B, Liao M, Sumiya M et al (2017) Nearly ideal vertical GaN Schottky barrier diodes with ultralow turn-on voltage and on-resistance. Appl Phys Express 10:051001
13. Johnson J, Zhang A, Luo W et al (2002) Breakdown voltage and reverse recovery characteristics of free-standing GaN Schottky rectifiers. IEEE Trans Electron Devices. 49:32-36
14. Zhou Y, Wang D, Ahyi C et al (2006) High breakdown voltage Schottky rectifier fabricated on bulk n-GaN substrate. Solid State Electron 50:1744–1747
15. Zhang L, Zhu J, Zhao M et al (2017) Fast recovery performance of vertical GaN Schottky barrier diodes on low-dislocation-density GaN substrates. Superlattice Microst 111:405–413
16. Matthews C, Flickera J, Kaplara R, et al. Switching characterization of vertical GaN PiN diodes. IEEE Workshop on Wide Bandgap Power Devices and Applications (WiPDA), 2016, 978: 135
17. Zhang X, Zou X, Tang C et al (2017) Switching performance of quasi-vertical GaN-based p-i-n diodes on Si. Phys Status Solidi A 214(8):1600817
18. Hsueha K, Cheng Y, Wang H et al (2017) Effect of AlN spacer layer thickness on AlGaN-GaN-Si Schottky barrier diodes. Mater Sci Semicond Process 66:69–73
19. Ueno K, Arakawa Y, Kobayashi A et al (2017) Highly conductive Ge-doped GaN epitaxial layers prepared by pulsed sputtering. Appl Phys Express 10(10):101002
20. Iwinska M, Takekawa N, Ivanov V et al (2017) Crystal growth of HVPE-GaN doped with germaniu. J Cryst Growth 480:102–107
21. Ajay A, Lim C, Browne D et al (2017) Effect of doping on the intersubband absorption in Si- and Ge-doped GaN/AlN heterostructures. Nanotechnology 28(40):405204
22. Nenstiel C, Bügler M, Callsen G, et al. Germanium-the superior dopant in n-type GaN. physica status solidi (RRL) - Rapid Research Letters, 2015, 9(12): 716–721
23. Liu X, Liu Q, Li C et al (2017) 1.2 kV GaN Schottky barrier diodes on free-standing GaN wafer using a CMOS-compatible contact material. Jpn J Appl Phys 56(2):026501
24. Gu H, Hu C, Wang J et al (2019) Vertical GaN Schottky barrier diodes on Ge-doped free-standing GaN substrates. J Alloys Compd 780:476–481
25. Takahide S, Shinya Y, Shinji N et al (2005) A study of correlation between traps and reverse-recovery characteristics of FWDs. In: Proceedings of the 17 international symposium on power semiconductor devices & IC's
26. Chiu H, Peng L, Wang H et al (2017) Improved reverse recovery characteristics of inAlN-GaN schottky barrier diode using a SOI substrate. Semicond Sci Technol 32:105009
27. Hsin Y, Ke T, Lee G et al (2012) A 600 V AlGaN/GaN Schottky barrier diode on silicon substrate with fast reverse recovery time. Phys Status Solidi C 9(3–4):949–952
28. Kang I, Kim S, Bahng W et al (2012) Accurate extraction method of reverse recovery time and stored charge for ultrafast diodes. IEEE Trans Power Electron 27(2):619
29. Tian F, Liu L, Gu H et al (2018) Investigation of the reverse recovery characteristics of vertical bulk GaN-based Schottky rectifiers. J Phys D Appl Phys 51:315101
30. Lee J, Park C, Im K et al (2013) AlGaN/GaN-based lateral-type Schottky barrier diode with very low reverse recovery charge at high temperature. IEEE transactions on power. electronics 60(10):3032